

Evaluating multi-loop Feynman diagrams with infrared and threshold singularities numerically

Charalampos Anastasiou

TH Unit, PH Department CERN, CH-1211 Geneva 23, Switzerland

E-mail: babis@cern.ch

Stefan Beerli and Alejandro Daleo

Institute for Theoretical Physics,ETH, CH-8093, Zurich, Switzerland

E-mail: sbeerli@itp.phys.ethz.ch

E-mail: adaleo@itp.phys.ethz.ch

ABSTRACT: We present a method to evaluate numerically Feynman diagrams directly from their Feynman parameters representation. We first disentangle overlapping singularities using sector decomposition. Threshold singularities are treated with an appropriate contour deformation. We have validated our technique comparing with recent analytic results for the $gg \rightarrow h$ two-loop amplitudes with heavy quarks and scalar quarks.

KEYWORDS: QCD, NLO and NNLO Computations.

1. Introduction

The evaluation of complicated Feynman diagrams remains one of the theoretical challenges to be met for the needs of the ongoing collider physics program. We develop an automated method to evaluate loop diagrams with infrared and threshold singularities in all kinematic regions. The method combines sector decomposition to simplify their infrared singular structures and a deformation of the integration path to treat threshold singularities.

Sector decomposition was introduced as a simple systematic algorithm to evaluate loop integrals by Binoth and Heinrich [1, 2]. The algorithm divides iteratively the integration region into sectors; in each sector the integration variables which could produce an overlapping singularity are ordered according to their magnitude. The overlapping singularity takes the form of a pole in the variable which approaches the singular limit first and can be factored out.

A concern for the viability of the method has been the proliferation of terms. In explicit calculations of cross-sections through next-to-next-to-leading order, it has been shown that one can write efficient sector decomposition algorithms for realistic applications in gauge field theories [3, 4, 5, 6, 7, 8]. However, to date, automated sector decomposition is limited to the calculation of infrared divergent loop diagrams in kinematic regions with trivial or no thresholds. This could halt progress in evaluating amplitudes for interesting scattering processes and fusion processes via heavy particles.

During the last few years an inspired method is being developed for the evaluation of one-loop amplitudes by Nagy and Soper [9, 10]. In their method, the infrared and ultra-violet divergences are matched algorithmically by simple counterterms for each diagram; these add up to functions which integrate to the known universal poles in ϵ of one-loop amplitudes. After the one-loop integrals are rendered finite in four dimensions, they perform a numerical integration over Feynman parameters and the loop momentum. They have proposed a systematic way to find an integration contour in the space of Feynman parameters which is suitable for a numerical integration.

We have merged the algorithm for sector decomposition with the contour deformation of Feynman parameters proposed by Nagy and Soper [10]. Since sector decomposition offers a general solution to rendering Feynman diagrams with divergences in $d \rightarrow 4$ dimensions finite, in principle, we can now compute generic multi-loop integrals numerically in all kinematic regions.

We have written three independent computer implementations of our method and performed extensive checks evaluating a variety of one and two-loop scalar and tensor integrals which we could verify with other methods. To prove the efficiency of our method, we have recomputed all diagrams in the two-loop amplitudes for $gg \rightarrow h$ production via heavy quarks and squarks, recently computed analytically. The new method yields numerical results which are in excellent agreement with the analytic evaluation [11].

Lazopoulos, Melnikov and Petriello have recently presented [12] the evaluation of the NLO QCD corrections to $pp \rightarrow ZZZ$. The method in their publication is the same as the one we are presenting. Here, we are applying it to the evaluation of a two-loop amplitude; together with the work of [12] this emphasizes further the versatility of the method.

Binoth et al. have used a contour deformation to evaluate integrals which are free of infrared divergences [13]. They also noted the possibility of merging sector decomposition and contour deformation as an alternative to their reduction method. To our understanding, the viability of this idea for practical applications was not investigated in [13].

A competitive numerical method for the evaluation of loop amplitudes is via Mellin-Barnes representations [14, 15]. Loop integrals with a small number of kinematic scales tend to have Mellin-Barnes representations with a lower dimensionality than the corresponding Feynman parameter representations. In such cases the Mellin-Barnes method should be advantageous; however, the method of this paper could perform better by increasing the number of kinematic scales. In addition, as noted in [15], Mellin-Barnes integrals cannot be computed stochastically in phase-space regions with mass dependent thresholds. For such applications the Mellin-Barnes method can be used only for checking purposes in the Euclidean region; sector decomposition with contour deformation could be then the only viable numerical method to obtain a physical result.

We should also note that a very significant progress in developing numerically integrable representations for two-loop three-point functions with threshold and infrared singularities has been made in [16]. However, this approach is yet not fully automated or general and requires an individual study for each topology.

We now present the method and our numerical results and comparisons.

2. Method

We first introduce independent Feynman parameters for a multi-loop Feynman diagram. In general, this yields a sum of terms of the form

$$I = C(\epsilon) \lim_{\delta \rightarrow 0} \int_0^1 dx_1 \cdots dx_n \frac{\mathcal{F}(\vec{x}, \epsilon)}{[\mathcal{G}(\vec{x}, M_i^2, s_{kl}) - i\delta]^{\alpha+n_L\epsilon}} \quad (2.1)$$

where α is an integer, n_L is the number of loops and M_i, s_{kl} are masses and kinematic invariants. The function \mathcal{G} is a polynomial of the independent Feynman parameters \vec{x} .

The integrand can be singular at the edges of the integration region. As a first step, we disentangle overlapping singularities using sector decomposition [17, 18, 1]. The outcome is a sum of integrals of the type

$$I_s = C(\epsilon) \lim_{\delta \rightarrow 0} \int_0^1 \frac{dx_1 \cdots dx_n x_1^{-\alpha_1+\beta_1\epsilon} \cdots x_n^{-\alpha_n+\beta_n\epsilon} \mathcal{F}_s(\vec{x}, \epsilon)}{[\mathcal{G}_s(\vec{x}, M_i^2, s_{kl}) - i\delta]^{\alpha+n_L\epsilon}} \quad (2.2)$$

The singularities at the edges of the integration region are now factorized. The function \mathcal{G}_s is finite at $x_i \rightarrow 0, 1$ and the singularities from the factors $x^{-\alpha+\beta\epsilon}$ when $\alpha > 0$ can be extracted independently for each integration variable. However, \mathcal{G}_s may produce singularities if it vanishes inside the integration region. It is important to postpone the extraction of the ϵ poles until we treat these threshold singularities first.

Following the method of Nagy and Soper [10], we construct a contour of integration where the imaginary part of \mathcal{G}_s is negative, that is, enforcing the $-i\delta$ prescription already

present in the original integral. The new contour is defined by deforming the integration path of every Feynman parameter; it is parameterized by

$$z_i = x_i - i\lambda x_i(1 - x_i) \frac{\partial \mathcal{G}_s}{\partial x_i}. \quad (2.3)$$

Provided that no poles were crossed in going from $[0, 1]$ to the contour C , we have

$$\int_0^1 \frac{\left(\prod_{j=1}^n dx_j x_j^{-\alpha_j + \beta_j \epsilon} \right) \mathcal{F}_s(\vec{x}, \epsilon)}{[\mathcal{G}_s(\vec{x}, M_i^2, s_{kl}) - i\delta]^{n_L \epsilon}} = \int_C \frac{\left(\prod_{j=1}^n dz_j z_j^{-\alpha_j + \beta_j \epsilon} \right) \mathcal{F}_s(\vec{z}, \epsilon)}{[\mathcal{G}_s(\vec{z}, M_i^2, s_{kl})]^{n_L \epsilon}}. \quad (2.4)$$

The choice of Eq. (2.3) for the contour deformation guarantees that for small values of λ , the function \mathcal{G}_s acquires a negative imaginary part of order $\mathcal{O}(\lambda)$

$$\mathcal{G}_s(\vec{z}) = \mathcal{G}_s(\vec{x}) - i\lambda \sum_i x_i(1 - x_i) \left(\frac{\partial \mathcal{G}_s}{\partial x_i} \right)^2 + \mathcal{O}(\lambda^2), \quad (2.5)$$

where the $\mathcal{O}(\lambda^2)$ terms are purely real. One could add higher order λ^n terms in Eq. (2.3) to cancel the imaginary parts of \mathcal{G}_s at $\mathcal{O}(\lambda^3)$ and higher orders. In practice, it is sufficient to perform a linear deformation as in Eq. (2.3), and choose a small enough value for λ such that these contributions are suppressed.

Changing variables using the parameterization in Eq. (2.3), each sector integral is now written as

$$\begin{aligned} I_s &= C(\epsilon) \int_0^1 \prod_{j=1}^n dx_j z_j^{-\alpha_j + \beta_j \epsilon} \mathcal{J}(\vec{x} \rightarrow \vec{z}) \mathcal{L}(\vec{z}(\vec{x}), \epsilon) \\ &= C(\epsilon) \int_0^1 \prod_{j=1}^n dx_j x_j^{-\alpha_j + \beta_j \epsilon} \left(\frac{z_j}{x_j} \right)^{-\alpha_j + \beta_j \epsilon} \mathcal{J}(\vec{x} \rightarrow \vec{z}) \mathcal{L}(\vec{z}(\vec{x}), \epsilon) \end{aligned} \quad (2.6)$$

where $\mathcal{J}(\vec{x} \rightarrow \vec{z})$ is the Jacobian of the transformation of Eq. (2.3). The function \mathcal{L} is finite in the boundary of the integration region and thus can be expanded as a Taylor series around $\epsilon = 0$. From Eq. (2.3) we can see that the ratios $z_i/x_i = 1 + \mathcal{O}(x_i)$ are also smooth in the singular limits.

Now, we are free to extract the ϵ poles in each integration variable by applying

$$\int_0^1 dx x^{-n+\epsilon} f(x) = \int_0^1 dx x^\epsilon \frac{f(x) - \sum_{k=0}^{n-1} x^k \frac{f^{(k)}(0)}{k!}}{x^n} + \sum_{k=0}^{n-1} \frac{f^{(k)}(0)}{k!(k+1-n+\epsilon)} \quad (2.7)$$

on Eq. (2.6). After this expansion, we are left with integrals which can be safely expanded in power series in ϵ . We compute the coefficients of the ϵ series numerically. Notice that in presence of higher order singularities, $n > 1$, the expansion in Eq. (2.7) involves derivatives of both the Jacobian and the function \mathcal{L} that contains all non-singular factors, including factors coming from the tensor structure of the integral.

There are many options for the numerical evaluation of the resulting integrals. For example, we can combine the contributions from all sectors into a single integrand; alternatively, we can integrate each sector separately and sum up the results. We have found that

the second choice is usually better, since the adaptation of numerical integration algorithms is more effective when dealing with simpler integrands.

We have implemented the method described above into three different programs. Sector decomposition and contour deformation are performed with MAPLE and MATHEMATICA routines. The same programs control the creation of numerical routines for the evaluation of the integrals; these are written in FORTRAN or C++. In all implementations we use the integration routines in the Cuba [19] library, relying mostly on the Cuhre and Divonne algorithms.

An important issue when performing the numerical integration is the value of the parameter λ in Eq. (2.3), which controls the magnitude of the contour deformation. A very small value could result to instabilities due to rounding errors. A very big value could result to a deformation with the wrong sign in Eq. (2.3). This last case is easy to detect at runtime and we have implemented diagnostic routines to abort the numerical evaluation if \mathcal{G}_s is found to have an imaginary part with the wrong sign. As we will show in the next section in an specific example, there is usually a very comfortable interval for λ where the result of the integration is insensitive to its value.

3. Results

We have applied our method to compute the two-loop amplitudes for $gg \rightarrow h$ mediated by a heavy quark or a scalar quark purely numerically. These amplitudes have been computed earlier either by using a mixture of analytic and numerical integrations [20, 21] or analytically in [11] and in [22]¹. We have evaluated all Feynman diagrams in these

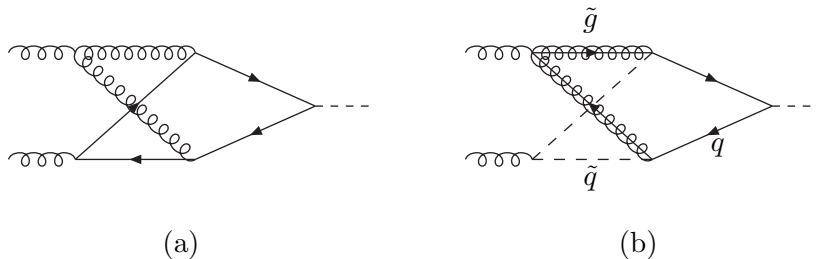


Figure 1: (a) Feynman diagram contributing to $gg \rightarrow h$ with a heavy quark loop. (b) Master integral arising in the calculation of $gg \rightarrow h$ in the MSSM.

amplitudes with a very good numerical precision. As an example, in Fig. 2 we show our results for the diagram in Fig. 1a. On the left panel we plot the real part of the finite piece of the diagram as a function of $\tau = s/(4m^2)$, normalized to $m^2 = 1$. The inset plot gives a more detailed view of the threshold region, where the numerical integration is most difficult, superimposed with the analytic results from [11]. The plot on the right panel shows the percent difference between the numerical result and the analytic one, normalized to the analytic value. In black lines we included the bands corresponding to the integration error, obtained by adding in quadrature the errors quoted by the integration routine for

¹The integral representation of the result in [20] was expressed in an analytic form in [23]

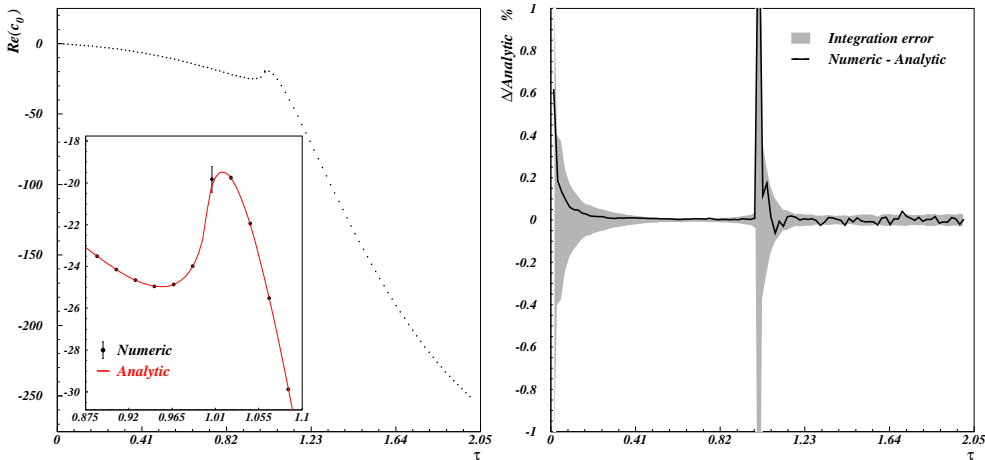


Figure 2: Results for the real part of the finite piece ($\text{Re}(c_0)$) of the Feynman diagram in Fig. 1a. The left panel shows the results of the numerical integration as black dots with error bars. The inset plot zooms in on the threshold region, the red line corresponds to the evaluation of the analytic result of [11]. The right panel shows the difference in percent of the numerical evaluation and the analytic one, normalized to the latter. The gray bands correspond to the integration error. At threshold this error is 3%.

each sector. We obtain similar results for the single pole and for the imaginary parts of both the single pole and the finite piece of this diagram.

As stressed above, the method relies on the proper choice of the value for the parameter λ . Values that are too large produce imaginary parts with the wrong sign for the function \mathcal{G}_s . Very small values generate a contour that is too close to the real line –and thus to the zeros of \mathcal{G}_s – and produce numerical instabilities. In practical implementations, we found that there is usually a good range for λ . As an example, in Fig. 3 we plot the results for the scalar integral corresponding to the diagram in Fig. 1a as a function of λ for two different values of τ . The results in these plots show that away from the threshold region, the integration is rather insensitive to the value of λ chosen, as long as it induces a deformation providing the right sign for the imaginary part in Eq. (2.5). On the other hand, close to the threshold region, the magnitude of the deformation has to be larger in order to get a reliable estimate of the integral.

As a novel result, we applied our method to the calculation of the scalar integral corresponding to the Feynman diagram of Fig. 1b. This integral is one of the master integrals appearing in the SUSY QCD corrections to $gg \rightarrow h$ and it involves a massive quark, a massive scalar quark and a massive gluino. Our results are displayed in Fig. 4 as a function of $\tau = s/(4m_q^2)$ for fixed values of $m_{\tilde{q}}^2 = 400/175 m_q^2$ and $m_{\tilde{g}}^2 = 600/175 m_q^2$ with $m_q = 1$. The results are again very stable over a wide range of λ . Due to the absence of massless propagators, the numerical evaluation of this integral turns out to be substantially faster than the scalar integral corresponding to the diagram of Fig. 1a.

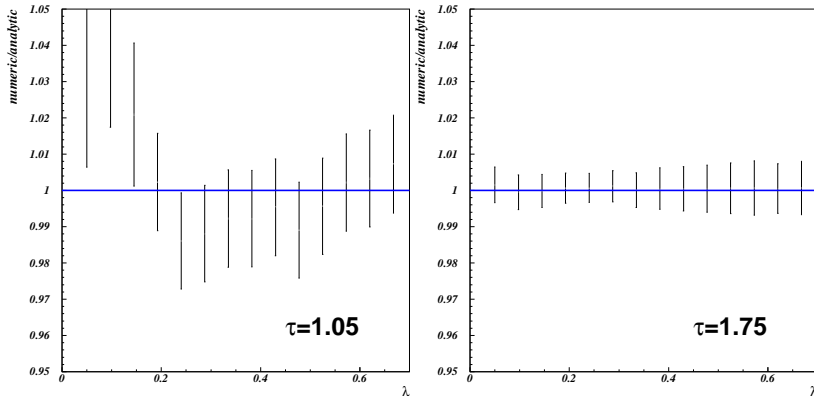


Figure 3: Results for the real part of the finite piece of the scalar integral corresponding to the Feynman diagram in Fig. 1a as a function of the parameter λ for two fixed values of the kinematical ratio τ . The results have been normalized to the analytic result for this master integral obtained in [11].

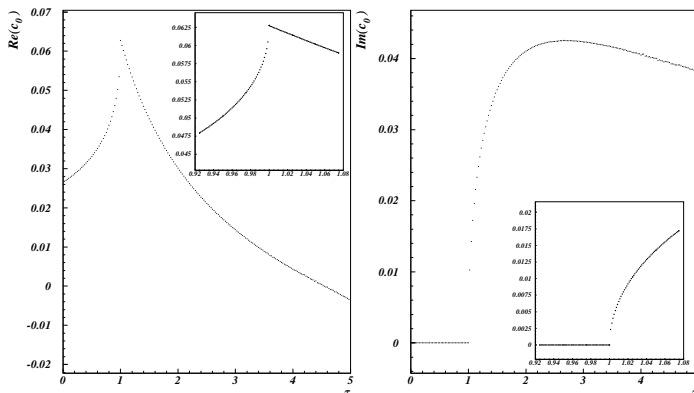


Figure 4: Results for the scalar integral corresponding to the Feynman diagram in Fig. 1b as a function of $\tau = s/(4m_q^2)$ for fixed values of $m_g^2 = 400/175 m_q^2$ and $m_q^2 = 600/175 m_q^2$. The inset plots zoom in the threshold region. The estimated relative accuracy of the points is better than 1 per mille.

4. Conclusions

We present a new method for the numerical evaluation of multi-loop Feynman diagrams containing both infrared and threshold singularities. The method uses sector decomposition to extract the infrared singularities followed by contour deformation in the Feynman parameters to deal with the thresholds present in the diagram. The algorithmic nature of the approach naturally leads to a high degree of automatization in all the stages of the calculation.

We tested the method recalculating the two loop corrections to $gg \rightarrow h$ mediated by a massive quark and a massive scalar quark. We find that the method is very efficient and

reliable, reproducing the analytic results with great accuracy.

Currently we are applying the technique to the calculation of the two loop SUSY QCD corrections to $gg \rightarrow h$. As an example, we have presented here results for one of the most complicated with analytical methods, yet uncalculated, master integrals appearing in this amplitude. We find excellent numerical behavior, showing that the framework has a great potential for computing automatically general multi-loop processes involving internal thresholds.

Acknowledgments

We are grateful to Uli Haisch and Zoltan Kunszt for many useful discussions and their encouragement. We thank Achilleas Lazopoulos, Kirill Melnikov and Frank Petriello for informing us of their publication [12] before submitting to the archive. The work of Stefan Beerli and Alejandro Daleo was supported by the Swiss National Science Foundation (SNF) under contract number 200020-113567/1.

References

- [1] T. Binoth and G. Heinrich, Nucl. Phys. B **585**, 741 (2000) [arXiv:hep-ph/0004013].
- [2] T. Binoth and G. Heinrich, Nucl. Phys. B **680**, 375 (2004) [arXiv:hep-ph/0305234].
- [3] K. Melnikov and F. Petriello, Phys. Rev. D **74**, 114017 (2006) [arXiv:hep-ph/0609070].
- [4] K. Melnikov and F. Petriello, Phys. Rev. Lett. **96**, 231803 (2006) [arXiv:hep-ph/0603182].
- [5] C. Anastasiou, K. Melnikov and F. Petriello, arXiv:hep-ph/0505069.
- [6] C. Anastasiou, K. Melnikov and F. Petriello, Nucl. Phys. B **724**, 197 (2005) [arXiv:hep-ph/0501130].
- [7] C. Anastasiou, K. Melnikov and F. Petriello, Phys. Rev. Lett. **93**, 262002 (2004) [arXiv:hep-ph/0409088].
- [8] C. Anastasiou, K. Melnikov and F. Petriello, Phys. Rev. Lett. **93**, 032002 (2004) [arXiv:hep-ph/0402280].
- [9] Z. Nagy and D. E. Soper, JHEP **0309**, 055 (2003) [arXiv:hep-ph/0308127].
- [10] Z. Nagy and D. E. Soper, Phys. Rev. D **74**, 093006 (2006) [arXiv:hep-ph/0610028].
- [11] C. Anastasiou, S. Beerli, S. Bucherer, A. Daleo and Z. Kunszt, JHEP **0701**, 082 (2007) [arXiv:hep-ph/0611236].
- [12] A. Lazopoulos, K. Melnikov and F. Petriello, arXiv:hep-ph/0703273.
- [13] T. Binoth, J. P. Guillet, G. Heinrich, E. Pilon and C. Schubert, JHEP **0510**, 015 (2005) [arXiv:hep-ph/0504267].
- [14] C. Anastasiou and A. Daleo, JHEP **0610**, 031 (2006) [arXiv:hep-ph/0511176].
- [15] M. Czakon, Comput. Phys. Commun. **175**, 559 (2006) [arXiv:hep-ph/0511200].
- [16] G. Passarino and S. Uccirati, Nucl. Phys. B **747**, 113 (2006) [arXiv:hep-ph/0603121].
- [17] K. Hepp, Commun. Math. Phys. **2**, 301 (1966).

- [18] M. Roth and A. Denner, Nucl. Phys. B **479**, 495 (1996) [arXiv:hep-ph/9605420].
- [19] T. Hahn, Comput. Phys. Commun. **168**, 78 (2005) [arXiv:hep-ph/0404043].
- [20] M. Spira, A. Djouadi, D. Graudenz and P. M. Zerwas, Nucl. Phys. B **453**, 17 (1995) [arXiv:hep-ph/9504378].
- [21] M. Muhlleitner and M. Spira, arXiv:hep-ph/0612254.
- [22] U. Aglietti, R. Bonciani, G. Degrossi and A. Vicini, JHEP **0701**, 021 (2007) [arXiv:hep-ph/0611266].
- [23] R. Harlander and P. Kant, JHEP **0512**, 015 (2005) [arXiv:hep-ph/0509189].